Advancing multifocal nonlinear microscopy: development and application of a novel multibeam Yb:KGd$(WO_4)_2$ oscillator

Kraig E. Sheetz,[1,*] Erich E. Hoover,[1] Ramón Carriles,[1] David Kleinfeld[2] and Jeff A. Squier[1]

[1]*Department of Physics, Colorado School of Mines, 1523 Illinois Street, Golden, Colorado 80401, USA*
[2]*Department of Physics, University of California, San Diego*
[*]*Corresponding author: ksheetz@mines.edu*

Abstract: We present a novel Yb:KGd$(WO_4)_2$ oscillator design that generates six beams of temporally delayed, 253 fs, 11 nJ pulses. This allows multifocal nonlinear microscopy to be performed without the need for complicated optical multiplexers. We demonstrate our design with twelve simultaneously acquired two-photon, second-harmonic and/or third-harmonic images generated from six laterally separated foci.

OCIS codes: (170.0180) Microscopy; (030.5260) Photon counting; (180.5810) Scanning microscopy; (180.4315) Nonlinear microscopy; (140.3480) Lasers, diode-pumped; (140.7090) Ultrafast lasers

References and links

1. V. Andresen, A. Egner, and S. W. Hell, "Time-multiplexed multifocal multiphoton microscope," Opt. Lett. **26**, 75-77, (2001).
2. N. Ji, J. Magee, and E. Betzig, "High-speed, low-photodamage nonlinear imaging using passive pulse splitters," Nat Meth **5**, 197-202 (2008).
3. M. Fricke and T. Nielsen, "Two-dimensional imaging without scanning by multifocal multiphoton microscopy," Appl. Opt. **44,** 2984-2988 (2005).
4. M. Straub and S. W. Hell, "Multifocal multiphoton microscopy: A fast and efficient tool for 3-D fluorescence imaging," Bioimaging **6**. 177-185 (1998).
5. K. Bahlmann, P. T. C. So, M. Kirber, R. Reich, B. Kosicki, W. McGonagle, and K. Bellve, "Multifocal multiphoton microscopy (MMM) at a frame rate beyond 600 Hz," Opt. Express **15**, 10991-10998 (2007).
6. J. Bewersdorf, R. Pick, and S. W. Hell, "Multifocal multiphoton microscopy," Opt. Lett. **23**, 655-657 (1998).
7. A. H. Buist, M. Muller, J. Squier, and G. J. Brakenhoff, "Real time two-photon absorption microscopy using multi point excitation," J. Microsc. **192**, 217-226 (1998).
8. D. N. Fittinghoff and J. Squier, "Time-decorrelated multifocal array for multiphoton microscopy and micromachining," Opt. Lett. **25**, 1213-1215 (2000).
9. K. H. Kim, C. Buehler, K. Bahlmann, T. Ragan, W. A. Lee, E. Nedivi, E. L. Heffer, S. Fantini, and P. T. C. So, "Multifocal multiphoton microscopy based on multianode photomultiplier tubes," Opt. Express **15**, 11658-11678 (2007).
10. W. Amir, R. Carriles, E. E. Hoover, T. A. Planchon, C. G. Durfee, and J. Squier "Simultaneous imaging of multiple focal planes using a two-photon scanning microscope," Opt. Lett. **32**, 1731-1733 (2007).
11. R. Carriles, K. E. Sheetz, E. E. Hoover, and J. Squier, "Simultaneous multifocal, multiphoton, photon counting microscopy," Opt. Express **16**, 10364-10371 (2008).
12. A. Major, R. Cisek, and V. Barzda, "Femtosecond Yb: KGd $(WO_4)_2$ laser oscillator pumped by a high power fiber-coupled diode laser module," Opt. Express **14**, 12163-12168 (2006).
13. F. Krausz, M. E. Fermann, T. Brabec, P. F. Curley, M. Hofer, M. H. Ober, C. Spielmann, E. Wintner, and A. J. Schmidt "Femtosecond solid-state lasers," IEEE J. Quantum Electron. **28**, 2097-2121 (1992).
14. D. N. Fittinghoff, C. B. Schaffer, E. Mazur, and J. Squier, "Time-decorrelated multifocal micromachining and trapping," IEEE J. Sel. Top. Quantum Electron. **7**, 559-566 (2001).
15. J. Squier and M. Müller, "High resolution nonlinear microscopy: A review of sources and methods for achieving optimal imaging," Rev. Sci. Instrum. **72**, 2855-2867 (2001).
16. Q. T. Nguyen and D. Kleinfeld, "Positive feedback in a brainstem tactile sensorimotor loop," Neuron **45**, 447-457 (2005).
17. W. Denk, J. H. Strickler, and W. W. Webb, "Two-photon laser scanning fluorescence microscopy," Science **248**, 73-76 (1990).

#101189 - $15.00 USD Received 5 Sep 2008; revised 8 Oct 2008; accepted 10 Oct 2008; published 16 Oct 2008

18. F. Helmchen and W. Denk, "New developments in multiphoton microscopy," Curr. Opin. Neurobiol. **12**, 593-601 (2002).

1. Introduction

In the past decade, significant progress has been made in the development of multifocal laser-scanning microscopes for use with two- and three-photon excited fluorescence and second- and third-harmonic imaging [1-9]. The goal of such systems is to reduce image acquisition times (without sacrificing resolution) in an effort to provide biologists and material scientists with a high-speed imaging capability for capturing processes in real time that yield valuable information about dynamical systems.

Most ultrafast laser systems used in nonlinear microscopy—typically Ti:Sapphire—generate peak pulse intensities well above the damage threshold for many biological samples. Thus the multifocal systems developed to date capitalize on this excess output power by splitting the single output beam into a one-dimensional or two-dimensional array of foci. Methods of creating multiple foci include microlens arrays [1, 4-7], etalons [8] and cascading beam splitters [2, 3]. For tightly spaced beam arrays, the foci must also be temporally offset to eliminate interference effects at the sample plane. While multifocal systems do allow for faster image acquisition rates, most do not provide information from multiple focal planes, which can be critical for imaging some dynamical processes.

We recently introduced a multifocal technique that is capable of imaging two focal planes simultaneously [10, 11]. This is accomplished by temporally demultiplexing the signal coming from two foci at different sample depths. The two foci are generated through an optical multiplexer that splits a single beam into two temporally delayed pulse trains, changes the divergence of one of them and recombines them into a collinear beam. In contrast to typical multifocal systems where the light generated from the individual foci within the sample is collected by a spatially-resolved imaging detector such as a charge coupled device (CCD) camera, our photon counting technique uses single-element detectors and is thus optimal for imaging through scattering media such as brain tissue. Scaling the system beyond two foci however, involved complex multiplexing optics.

In this work we report the design and construction of, to our knowledge, the first laser that generates an array of six time decorrelated, laterally displaced foci directly from the oscillator cavity. We apply this multibeam laser to multifocal, nonlinear microscopy, thus eliminating the need for complex multiplexing optics and overcoming the scaling limitation of our two foci system. Figure 1 shows a simple block diagram illustrating the simplification realized by the design of our novel extended cavity 18.6 MHz Yb:KGd$(WO_4)_2$ (Yb:KGW) oscillator configured to generate six time-delayed output beams per cavity round trip. Under stable mode lock conditions, the oscillator produces bursts of six 253 fs pulses with 6 ns inter-pulse spacing, centered at 1039 nm, and having average energies of up to 11 nJ/pulse.

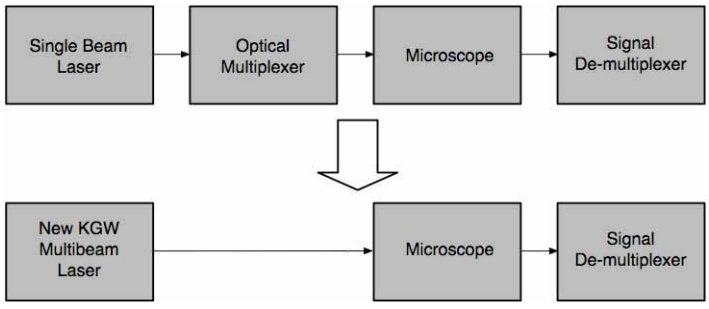

Fig. 1. Block diagram showing the simplification realized with the Yb:KGW multibeam laser design for nonlinear microscopy.

#101189 - $15.00 USD Received 5 Sep 2008; revised 8 Oct 2008; accepted 10 Oct 2008; published 16 Oct 2008

Coupling this unique oscillator design with our temporal demultiplexing system, we simultaneously recorded two nonlinear modalities, selected from two-photon excited fluorescence (TPEF), second harmonic generation (SHG) and third harmonic generation (THG), from each of the six foci to obtain a total of 12 simultaneously acquired images. In the following sections, we describe the oscillator design and output characteristics, as well as the technique to relay multiple foci to the sample plane in a scanning configuration. Additionally, we briefly discuss signal demultiplexing and image acquisition electronics and provide two sets of images to demonstrate the system capability and limitations.

2. Experimental setup

2.1 Oscillator design and characteristics

Our multibeam Yb:KGW oscillator design (Fig. 2) is based on a single-output-beam femtosecond Yb:KGW laser developed by Major et al. [12]. The pump source is a 25W fiber-coupled diode module with a 200-μm core diameter emitting at 980 nm (F25-980-2, Apollo Instruments, Inc). The fiber output is imaged 1:1 (LL60 lens assembly, Apollo Instruments, Inc) into a 4-mm long, 5-mm wide and 5-mm thick AR-coated 5% Yb:KGW crystal (Eksma). The pump light enters the cavity through a short wave pass flat mirror, M3, coated for 98% transmission at the pump wavelength and 99.9% reflection at the laser wavelength. The crystal is cooled to 15° C by a thermoelectric cooler (TE Technology, Inc) and a water-cooled copper crystal mount of local design.

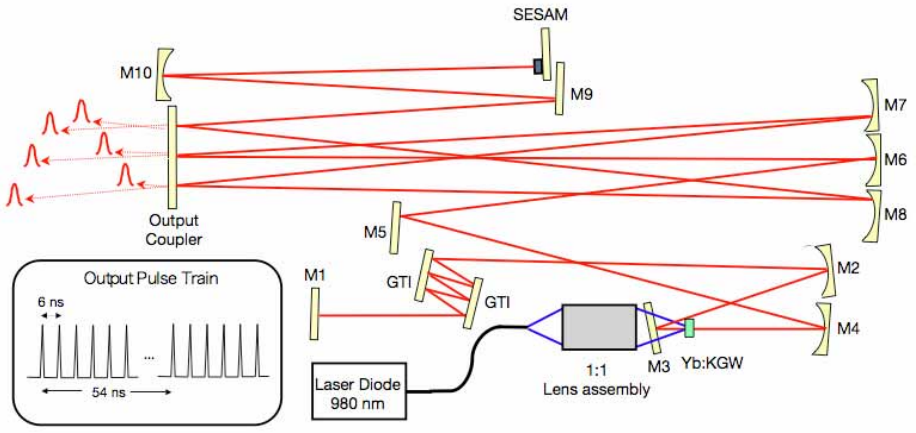

Fig. 2. Schematic representation of Yb:KGW oscillator layout. Mirrors are labeled by M1-M10, Gire-Tournois interferometer mirrors by GTI, and semiconductor saturable absorber mirror by SESAM. The laser cavity footprint is 125 cm by 50 cm.

In the short arm of the cavity we have a highly reflective (HR, >99.98%) flat mirror, M1 (Layertec, GmbH), a pair of Gires-Tournois interferometer (GTI) mirrors (Layertec, GmbH) that provide -1300 fs^2 per bounce with six bounces per mirror per round trip, and a curved HR mirror, M2 with a radius of curvature r = 200 mm (Layertec, GmbH). The long arm of the cavity starts with another 200-mm curved mirror, M4 (Layertec, GmbH). Two flat HR mirrors, M5 and M9 (Layertec, GmbH) are used to fold the laser light into and out of a unique cavity extension that uses three curved HR mirrors, M6, M7 and M8 (r = 2 m, Layertec, GmbH) to generate six bounces per round trip from a two-inch diameter, 1% output coupler (CVI, Inc). Mode locking is achieved by focusing the beam with a curved HR mirror (r = 500 mm, Layertec, GmbH) onto a semiconductor saturable absorber (SAM-1040-2-25.4g, Batop, GmbH) with a modulation depth of 1.2%. A light tap on the optical table is usually sufficient to mode lock the laser at start-up.

#101189 - $15.00 USD Received 5 Sep 2008; revised 8 Oct 2008; accepted 10 Oct 2008; published 16 Oct 2008

At maximum pump power, the average power in each of the six output beams ranges from 335 to 365 mW, depending on the output coupler bounce sequence relative to the gain medium. However, pulse splitting due to excessive self-phase modulation tends to occur at average powers above ~250 mW. In our oscillator development, we observed the mode lock stability dependence on the interplay between self-phase modulation in the crystal and intracavity negative dispersion [13] and found that we could increase the average power at stable mode lock by increasing the negative dispersion in the cavity via more bounces off of the GTI mirror pair. With the current configuration of six bounces per round trip, we found the most stable mode lock region to be between 125 and 200 mW average output power (per beam). Given our total cavity repetition rate of 18.6 MHz, this corresponds to average pulse energies of 7-11 nJ which is more than sufficient for most imaging applications. The generated pulses are centered at 1039 nm and have a bandwidth of 4.7 nm FWHM. Our oscillator design does not permit central wavelength tunability. The pulse duration, as measured with a second-order intensity autocorrelator, is 253 fs. The time-bandwidth product is thus calculated to be 0.330 compared to 0.315 for a transform limited pulse assuming a sech^2-shaped temporal profile.

The inset of Fig. 2 shows the resulting temporally separated pulse train as measured by a photodiode. Given the cavity geometry, the delay between the six foci generated each round trip is 6 ns and the six-pulse bursts are temporally separated by 54 ns (18.6 MHz).

2.2 Multifocal scan optics

In order to apply the six-output-beam oscillator to scanning multifocal microscopy, the optical system shown in figure 3 was developed to take a one-dimensional array of collimated beams, magnify them, and overlap them at slightly different angles at the entrance aperture of a microscope objective (see magnified inset of Fig. 3). The system is arrayed so that the focus of the six beams on the horizontal scan mirror is imaged to the entrance aperture of the objective in such a way that the beams slightly overfill the objective aperture and can be scanned in two dimensions without vignetting [8].

Although the folding angles in the cavity extension were minimized to the greatest extent possible, the pulses are not co-linear and exit the cavity at various angles relative to the face of the output coupler (Fig. 2). One four-inch silver mirror was placed directly after the output coupler to turn the beams toward six ¼-inch silver mirrors that turn the beams to form a one-dimensional array of six ~1-mm diameter parallel beams with 5-mm inter-beam separation. The focal lengths and positions of the five lenses and scan mirrors in the scan optics system were determined by starting with the theoretical treatment of imaging multiple beamlets to an objective presented by Fittinghoff et al. [14] and refining the parameters with a paraxial ray tracing program. All lenses are achromatic doublets designed and coated for 1 μm light (CVI, Inc). The first lens, L1, has a two-inch aperture and a focal length of 750 mm and focuses the beams onto the first of two 5-mm clear aperture galvanometric scan mirrors (driven by SC2000, GSI Group, Inc). The focal point of L1 forms the first of three telecentric planes in the optical system. Lenses L2 and L3 are one-inch in aperture lenses with focal lengths of 40 mm and form a 1:1 telescope to image the telecentric plane from the first scan mirror to the second scan mirror. Lens L4 has a ½-inch aperture and a focal length of 19 mm. This lens serves to return the axes of the beams to a parallel configuration while sharply focusing the individual beams so that they can expand to a diameter that will overfill the objective. Lens L5 is a one-inch, 100 mm tube lens that re-collimates the individual magnified, beams and overlaps the six beams to the third telecentric plane at the entrance aperture of the objective.

#101189 - $15.00 USD Received 5 Sep 2008; revised 8 Oct 2008; accepted 10 Oct 2008; published 16 Oct 2008

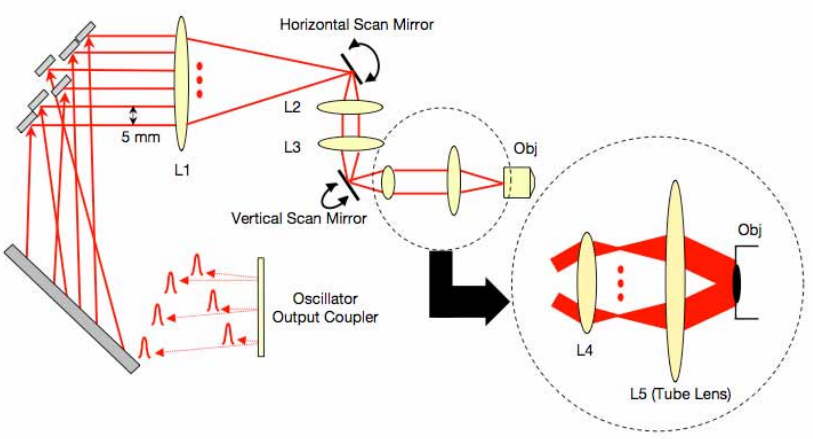

Fig. 3. Schematic representation of multifocal scan optics. Achromatic doublets are labeled L1-L5. Magnified inset shows beam configuration on back pupil of objective required for scanning. Central beams are omitted for clarity.

To test the scan optics and to make minor adjustments to the one-dimensional six-beam array via the ¼-inch turning mirrors (Fig. 3), we placed a thin cell of Rhodamine-6G at the focal plane of the objective and imaged the two-photon fluorescence from the six foci at the four corners of various-sized scan areas onto a CCD camera. Figure 4 shows a sample overlay of four two-photon fluorescence images taken at the corners of an 88 µm by 88 µm scan area with a Zeiss A-plan 40×, 0.65 NA objective. Our scanning configuration can support a scan area, i.e., field of view, of ~130 µm by 130 µm before vignetting clips the outer beams of the array; the six-beam array has a lateral extent of ~30 µm.

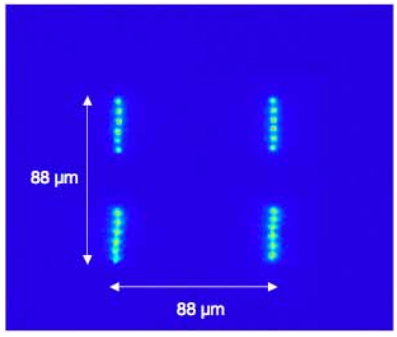

Fig. 4. Four corners of an 88 µm by 88 µm scan area for the six-foci system. Image shows overlaid CCD screen captures of two-photon fluorescence from Rhodamine-6G sample. Objective was a Zeiss A-plan 40×, 0.65 NA.

2.3 Characterization of the foci

The ray-tracing models used to develop the scan optics system discussed above assume that the individual Gaussian beams are all collimated prior to lens L1 (Fig. 3) and thus returned to a collimated state (albeit expanded) upon combination at the entrance aperture of the objective. However, in our system we do not collimate the individual beams prior to the scan optics but rather leave them in the slow divergence state they have upon exit from the laser cavity. Since each beam is coupled out of the cavity at a different time within the round trip period, the mode for each beam has slightly different divergence characteristics.

#101189 - $15.00 USD Received 5 Sep 2008; revised 8 Oct 2008; accepted 10 Oct 2008; published 16 Oct 2008

Table 1. Axial resolution and axial offset for each of the six beams. Axial offset is relative to the first focusing (shallowest) beam (beam 4).

Beam	Measured axial resolution (μm)	Axial offset from shallowest focusing beam (μm)
1	6.7	1.0
2	6.6	0.9
3	7.0	1.2
4	6.3	0
5	6.5	0.5
6	6.5	0.4

To measure the relative focal plane separation along with the axial resolution of each the six beams when focused with our 0.65 NA objective, the beams were individually focused into a sample of Rhodamine-6G while blocking all but one beam for each measurement. The two-photon excited fluorescence signal was detected by a photomultiplier tube (Hamamatsu R7400-U4) as the sample was translated axially by a computer-controlled stage. The measured depth of focus and relative axial focal position listed in Table 1 and shown graphically in Fig. 5 indicate a focal plane offset of only 1.2 μm as a direct consequence of oscillator geometry. Note that in Fig. 5, the axial dimension (z) is stretched relative to the beam array dimension for clarity; however, lengths along the z-axis are roughly to scale and illustrate the fact that the total focal plane offset of 1.2 μm is negligible in comparison to the diffraction-limited value for the axial resolution [15] of $z_0 = 2n\lambda/(NA)^2 = 6.4$ μm. The measured lateral resolution of each beam was 1.0 μm which matches the diffraction-limited value [15] of $r_0 = 2\lambda/NA = 0.98$ μm.

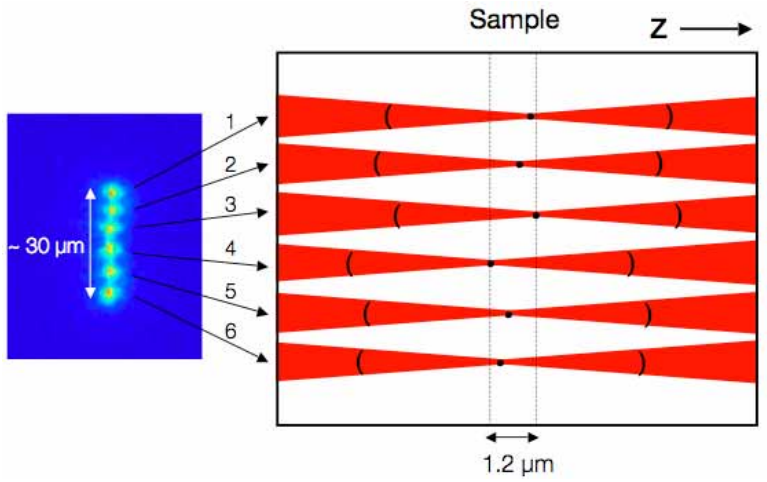

Fig. 5. Graphical portrayal of foci geometry in a sample. Axial dimension (z) is stretched relative to lateral dimension for clarity. The depth of focus is indicated by curved black lines on the focusing beam and the offset of the center of focus is marked by black dot. Beams are numbered top to bottom as arrayed in the CCD image capture.

#101189 - $15.00 USD Received 5 Sep 2008; revised 8 Oct 2008; accepted 10 Oct 2008; published 16 Oct 2008

2.4 Multimodal microscope configuration

Figure 6 shows a schematic of the setup for multimodal detection in our microscope. The microscope is configured to collect TPEF in the epi direction and SHG and THG in the transmitted direction. A combination of a 2-mm thick dichroic that reflects the wavelengths between 350 nm and 700 nm and transmits above 800 nm, and a 3-mm thick long-pass filter at 540 nm is used to separate the TPEF signal from the excitation beam and any harmonics before detection with a photomultiplier tube (PMT) (Hamamatsu R7400-U4). To detect THG, we use a 5-mm thick harmonic separator that reflects a 40 nm bandwidth centered on 355 nm to a UG-11 filter and a PMT (Hamamatsu R7400U-04. Lastly, to detect SHG, we filter the transmitted light with an interference filter centered at 520 nm and use a PMT (Hamamatsu R7400P) for SHG detection. All three detection arms also have a colored glass filter (3 mm, BG39) to remove light at the fundamental wavelength. Additionally, we have two flipper mirrors in place to capture white light images of the sample region of interest on a CCD camera.

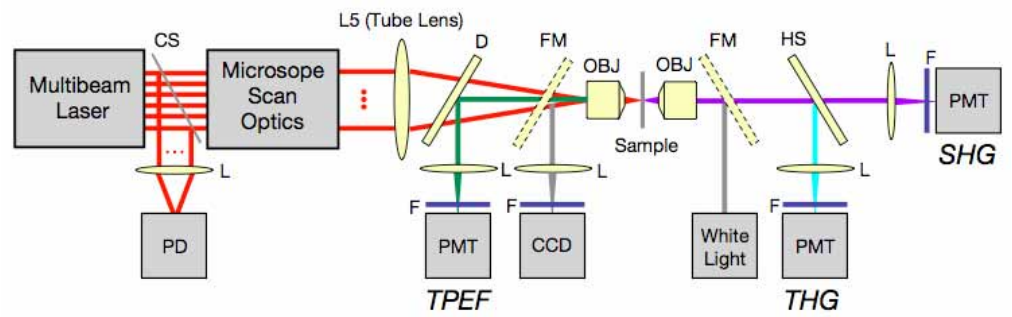

Fig. 6. Schematic representation of the experimental setup (not to scale): D, dichroic mirror; HS, harmonic separator; CS, 190 µm-thick coverslip; F, interference and/or color glass filters; FM, flipper mirrors; FL, focusing lenses (f = 50 mm); PD, photodiode; PMT, photomultiplier tube; CCD, CCD camera; OBJ, objective lens. The photodiode is used to provide a laser clock for electronic demultiplexing. The flipper mirrors are used to obtain white light images of the sample region of interest. Details of the multibeam laser and microscope scan optics are in Figs. 2 and 3 respectively.

2.5 Simultaneous multifocal photon counting electronics

The photon counting imaging electronics used in this work are a direct extension of our previously reported simultaneous multiphoton, photon counting system for two foci [10, 11]. The signal produced by each of the six foci is separated based on its relative timing with respect to the laser pulses as monitored with a photodiode (Fig. 6). A demultiplexer and six counters are programmed into a field programmable gate array (FPGA, Altera DE2) card. The demultiplexer toggles between each counter with every laser pulse from the photodiode. Each 16-bit counter thus stores the photon count from a single focus. The photon count is recorded to onboard memory and reset to zero each time the FPGA receives a signal marking the end of the pixel dwell time generated by the scan mirror controller. At the end of each scan, the stored values are sent to a computer over a USB port, where the intensity images coming from each of the six foci are generated and displayed. A more detailed description of the FPGA software and hardware architecture of this quantitative tool for photon counting nonlinear microscopy is given in Refs. [10, 11].

#101189 - $15.00 USD Received 5 Sep 2008; revised 8 Oct 2008; accepted 10 Oct 2008; published 16 Oct 2008

3. Imaging results: demonstration of system capabilities and limitations

Our current image acquisition capability enables us to acquire twelve images simultaneously—six images from any two of the three modalities for which the microscope is configured (Fig. 6). In order to obtain two sets of six images we split the laser clock, pixel clock and line synchronization signals to two identical FPGAs, and connect one PMT to each card. The computer program that handles the communications with the FPGA boards can control two boards simultaneously. We are currently modifying the computer program and electronics to control three boards and enable the acquisition of 18 images simultaneously, i.e., six each of TPEF, SHG, and THG. All images presented in this report are raw data. No background subtraction was performed in any of the images.

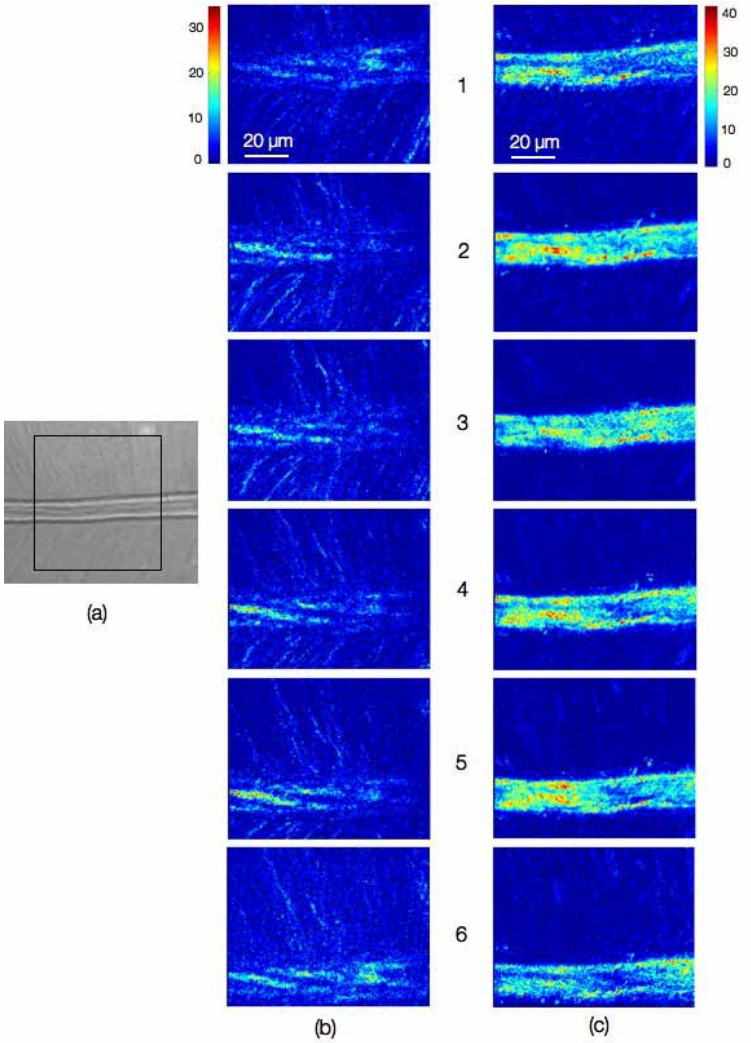

Fig. 7. Twelve simultaneously acquired images of trigeminal nerve from the adult mouse sectioned at 50 μm. Panel (a) shows a white light image of the region of interest; field of view denoted by black box. Panels (b) and (c) are SHG and THG images respectively generated at each of the six foci; beam numbers between panels correspond to numbering shown in Fig. 6. Images are 128 × 128 pixels; photon count scales shown with image 1 apply to all images in the respective column. A Zeiss A-plan 40×, 0.65 NA objective was used for excitation and a New Focus Aspheric lens, 60x, 0.65 NA was used for collection; the acquisition time was 10 s.

#101189 - $15.00 USD Received 5 Sep 2008; revised 8 Oct 2008; accepted 10 Oct 2008; published 16 Oct 2008

We used a 50-μm thick section of the fixed trigeminal nerve that was dissected from adult mouse [16] fixed, and mounted between a microscope slide and a coverslip with ProLong-Gold-Antifade-Reagentwater-based mountant (Invitrogen, CA). This provided an excellent test sample to demonstrate the multimodal, multifocal imaging capability of the system. Figure 7 shows twelve simultaneously acquired 128 x 128-pixel images—six SHG images and six THG images. Both modalities were collected in transmission. Panel (a) shows a white light image of the region of interest. Panel (b) shows six SHG images (one for each of the six foci) and panel (c) shows six THG images. The numbers in the center column link the images to the beam numbers as established in Fig. 6. Note that the fields of view of the first and the sixth images are displaced by ~30 μm, which corresponds to the lateral separation between the end foci in the beam array. The color scale accompanying each figure is given in photons per pixel. In this case the total image acquisition time was 10 s yielding a pixel dwell time of approximately 610 μs. Given that the pulse energy at the sample plane (ND filtered to ~1 nJ per pulse) for this data set is an order of magnitude less than the available energy within the stable mode lock regime, this system shows great promise for high-speed imaging applications.

The pulses from our multifocal laser are temporally separated by 6 ns (see inset of Fig. 2) as dictated by the oscillator geometry. As mentioned above and in Refs [10, 11], our demultiplexing electronics generate images by binning signal photons where the bin for each focus stays open for 6 ns. For instantaneously generated harmonics, i.e., SHG and THG, the signal will always be attributed to the appropriate focus (the bin opens upon detection of the rising edge of the laser clock pulse). However, there is a noteworthy limitation when detecting TPEF signals. Fluorescent molecules have an intrinsic fluorescence lifetime distribution that can extend to many nanoseconds [17, 18]. For molecules with lifetime distributions that reach into the several nanosecond regime, signal photons from a given laser pulse could be assigned to the bin corresponding to the subsequent laser pulse.

To illustrate the above effect, we created a sample consisting of cornstarch granules (dry cornstarch purchased from local grocer), which are strong SHG emitters, and 10-μm diameter polystyrene crimson fluorescent microspheres (Invitrogen, CA), which are strong TPEF emitters, mounted between coverslips. We recorded a set of images with five of the six beams blocked right after the coverslip that directs the beams to the photodiode (between the coverslip, CS, and the microscope scan optics in Fig. 6). Only beam two was actually incident on the sample; the demultiplexing electronics generated images for all six foci. Figure 8 shows eight of twelve simultaneously acquired images of a cornstarch granule surrounded by fluorescent microspheres. Panel (a) shows a white light image of the region of interest. Panel (b) shows four SHG images (for foci 1-4; images 5-6 did not differ visibly from image 4) and panel (c) shows four TPEF images (also for foci 1-4). The photon-count scale on the images associated with foci 1, 3 and 4 is reduced by an order of magnitude relative to the image associated with focus 2 in order to demonstrate a system capability and a limitation. Clearly the cornstarch granule only appears in the SHG image and the microspheres only appear in the TPEF image, thus highlighting the ability to acquire multimodal images simultaneously that can discriminate between features within the field of view. Additionally, the SHG image of the cornstarch only appears in the frame associated with beam 2, thus verifying the capability of the electronics to appropriately bin the signal photons. However, 3 to 4 % of the TPEF signal photons from the microspheres bled into the frame associated with beam 3. In other words, as a result of fluorescence lifetime, the 6-ns bin width is occasionally exceeded and the electronics therefore attribute those photons to the wrong beam. For standard TPEF imaging, this represents a limitation that will have to be calibrated and corrected for before using images for any quantitative analysis.

#101189 - $15.00 USD Received 5 Sep 2008; revised 8 Oct 2008; accepted 10 Oct 2008; published 16 Oct 2008

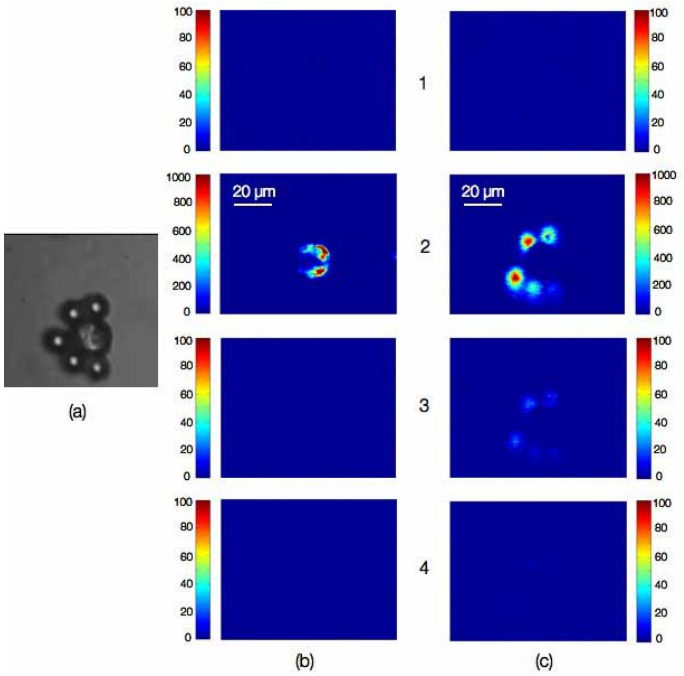

Fig. 8. Eight of twelve simultaneously acquired images of a corn starch granule surrounded by fluorescent microspheres; image pairs 5 and 6 do not differ from 4. All beams except beam 2 are blocked just prior to the objective lens. Panel (a) shows a white light image of the region of interest. Panels (b) and (c) are SHG and TPEF images, respectively, attributed to the first four foci; beam numbers between panels correspond to numbering shown in Fig. 6. Images are 128 × 128 pixels, Zeiss A-plan 40×, 0.65 NA objectives were used for excitation and collection; the acquisition time was 10 s.

4. Conclusion

We have developed a novel multibeam laser that generates an array of six high energy beams of temporally separated femtosecond pulses and overcomes a scaling limitation of our previous temporally separated multifocal system. Using the multibeam laser in conjunction with our simultaneous multifocal, multiphoton photon counting image acquisition system that uses field programmable gate arrays to demultiplex the signals, we have simultaneously acquired twelve multimodal images from six laterally separated foci: six SHG images, one per focus, and six THG images. This marks a unique step in the advancement of multifocal, nonlinear microscopy toward real-time 3-D imaging.

In the current configuration, the six laterally separated beams all focus to the same (within ~1 µm) focal plane. Although this clearly increases the total field of view achieved for a given scan time, the system has unique application beyond decreasing static image acquisition times. One such application is the ability to access multiple channels in parallel inside of a microfluidic system.

Future modifications to the system include optics to "tune" the divergence of the individual beams external to the oscillator and thus vary the axial offset of the focal planes within the sample. For example, by offsetting the six foci in 10 µm steps and scanning a 100 µm x 100 µm lateral area, biologists could simultaneously image six planes in a 100 µm x 100 µm x 50 µm volume. Once a region of interest is identified, the focal offset could be reduced to eliminate axial dead space and capture dynamic processes such as blood flow or cellular dynamics. We are currently exploring methods to achieve tunable axial offset such as reflecting the beam array off of a small-element deformable mirror that can independently affect the divergence of each beam, or inserting small-lens telescopes into the pathway of each beam prior to the scan optics. In the first case, the deformable mirror could be actively

#101189 - $15.00 USD Received 5 Sep 2008; revised 8 Oct 2008; accepted 10 Oct 2008; published 16 Oct 2008

programmed to tune the axial offset. In the latter case, the inter-lens spacing of the telescopes could be changed to tune the axial offset. Regardless of the method employed, an imaging system that can rapidly scan an array of laterally and axially offset foci will provide biologists with a powerful tool for capturing important processes in dynamical systems.

Acknowledgments

We thank Virginijus Barzda and Arkady Major for fruitful discussions on extended cavity KGW oscillator design and Rodolfo Figueroa for preparing the nerve sample. This work was partially supported by a National Institutes of Health Bioengineering Research Partnership (grant EB003832).

#101189 - $15.00 USD Received 5 Sep 2008; revised 8 Oct 2008; accepted 10 Oct 2008; published 16 Oct 2008